Iran University of Science and Technology

International Journal of Automotive Engineering

Journal Homepage: ijae.iust.ac.ir

ISSN: 2008-9899

Rollover avoidance in sport utility vehicles: a multi-criteria viewpoint

Javad Rezapour[1*], Parvaneh Afzali[2]

[1] Department of Mechanical Engineering, Lahijan Branch, Islamic Azad University, Lahijan, Iran.

[2] Department of Software Engineering, Astaneh Ashrafieh Branch, Islamic Azad University, Astaneh Ashrafieh, Iran.

ARTICLE INFO

Article history:

Received: 7 May 2020

Accepted: 22 Aug 2020

Published: 1 Sep 2020

Keywords:

Artificial intelligence

Lateral instability

Multi-criteria optimization

Sliding control theory

A B S T R A C T

Rollover of sport utility vehicles is a critical challenge for dynamic stability of the vehicle. Due to the high rate of fatalities resulted from the rollover, in order to reduces the injuries, the design of active vehicle controllers has received significant attention among the researchers and car companies. In this article, a multi-criteria optimum method is discussed in order to design a dynamics stabilizing controller via differential braking with an optimum braking torque distribution. To this end, the nonlinear control method on the basis of the sliding mode techniques has been implemented that provides ride comfort, improve safety performance, and maintain maneuverability. To address the trade-off between the challenge issue in these systems in terms of maneuverability and rollover prevention capability, we formulate an artificial intelligence-based multi-criteria genetic algorithms. The simulation verification analysis indicates that the utilized optimum distribution braking torques result in the desired enhancement in roll stability of the vehicle.

1. Introduction

Lateral dynamic instability of vehicle-type rollover is the most important issue in the field of transportation and its safety has attracted the attention of many researches. The rollover accidents are divided into two parts as tripped and untripped rollovers.

The tripped rollover happens because of the side collision to an external obstacle, for example: the curb, pothole, or guardrail. The untripped rollover, usually, is happened due to driving maneuvers vehicle goes out of balance and rolls over [1]. Over the past decades, the increased popularity of sport utility vehicles (SUVs) with higher center of gravity (C.G.) than sedans has persuaded academic researchers to study the potential improvements in rollover protection and also the governmental agencies and car companies to look at manufacturing orders precisely, aiming to reducing mortalities due to

*Corresponding Author
Email Address: Rezapour@liau.ac.ir
https://doi.org/10.22068/ase.2020.544

[DOI: 10.22068/ase.2020.544]

expense of fabricating and manufacturing, by considering higher rollover tendency. Reports of national highway traffic safety administration (NHTSA) show that rollover leads to severe and fatal crashes of road accidents and the rollover accidents are estimated to be the most dangerous form of accident, after head-on collisions [2]. The similar analysis for vehicle rollover were reported in [3 to 5]. Therefore, it is necessary to avoid rollover of vehicle. However, many inquiries have been done. For instance, Anwar proposed a developed theoretical and practical result of a vehicle shift to stability control system in case of generalized predictive control (GPC) method [6 and 7]. Wang presented a design for demand dependent active suspension consist of four double direction hydraulic actuators, hydraulically interconnected which seriously lean the vehicle against its roll direction by providing an essential restoring moment [8]. In order to improve the safety and longitudinal stability of a vehicle equipped with standard ABS system, an adaptive modified fuzzy-sliding mode longitudinal control design and simulation for vehicles equipped with ABS system was presented by [9]. Design of an Adaptive Fuzzy Controller for Antilock Brake Systems was proposed in [10] because of the nonlinearity of the vehicle dynamic model, three fuzzy-estimators have been suggested to eliminate nonlinear terms of the front and rear wheels' dynamic. Cairano considered a system where active front steering and differential braking are available and proposed a model predictive control (MPC) method to coordinate the actuators [11]. Also, Doumiati used similar method by using a suitable gain scheduled linear parameter varying (LPV) controller to ensure vehicle stability [12]. Additionally, a wide range of investigations in the literature has been developed to reduce or prevent rollover threat [13 and 14].

Hence, rollover is of the utmost importance in designing an active safe control system, and as such is valuable of further scientific study. In order to simplify the control design and tuning procedures, to the best of authors knowledge, the existing references in the literature are limited to the linearized equations of motion for up to four degrees of freedom (DOF), for example [14 to 21]. This simplification essentially results in modeling errors comparing to the high order nonlinear model of the vehicle.

in this study, we suggest a complete vehicle model for the purpose of rollover stability analysis. This model includes eight DOF model for equations of motion, nonlinear combined slip tire model, and two-track chassis model of vehicle. Sliding mode control (SMC) is designed for lateral stabilization of the model. Although the SMC theory results in a reliable control system, many parameters should be tuned to achieve the desired goals in practice. Therefore, we adopt the multi-objective uniform-diversity genetic algorithm (MUGA) with a diversity preserving mechanism (called the ε-elimination algorithm) for Pareto optimization of controller parameters. Absolute area under the curve of roll angle over time and area under the curve of total braking torque over time are the objective functions used for minimization. The design variables that are used in the optimization, are all seven parameters of our SMC algorithm. Utilizing Pareto fronts obtained by MUGA process, a trade-off optimum design can be confirmed. Through the obtained numerical results, it is found that the utilized optimum distribution braking torques can result in obtaining desired enhancement in roll stability and maneuverability.

The residual of the article is organized in this way. First, we develop an eight-DOF model for rollover simulation. Then the structure of the controller system for avoiding the rollover of the simulation is designed and formulated. Also, the multi-objective tuning method to find the optimum parameter values for our sliding controller is proposed. The simulation results and discussions are presented next. Finally, the conclusion and summary are given.

2. System modeling

Figure 1 shows a schematic view of the dynamic model of an eight-DOF system in planar model.

[DOI: 10.22068/ase.2020.544]

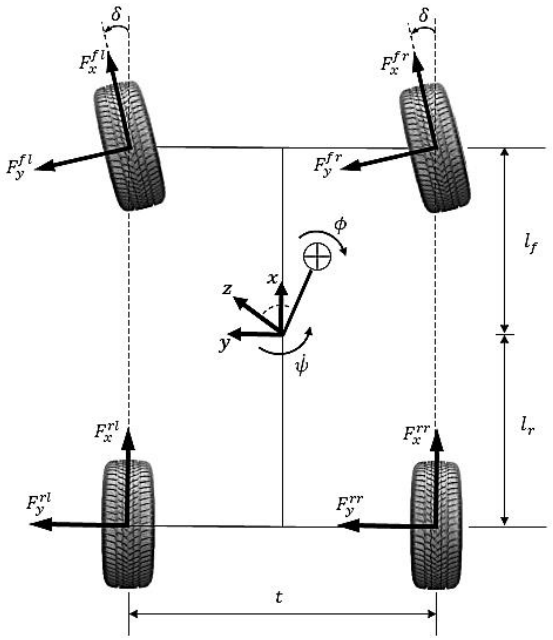

Figure 1: Typical view of the vehicle model with roll dynamics

Figure 2 displays the suspension system of the model. In this figure, C_φ and K_φ denote the roll damping and stiffness coefficients, respectively. It should be noted that in the present modeling, the pitch angle (rotation around y axis) is neglected in order to study the behavior breaking system based on four-wheel rotation as demonstrated in Figure 3. The exhibited model has eight degrees of freedom which are considered to be the rotational speed of the wheels, translational motions along x and y axis, and rotations around x (roll) and z (yaw) axis.

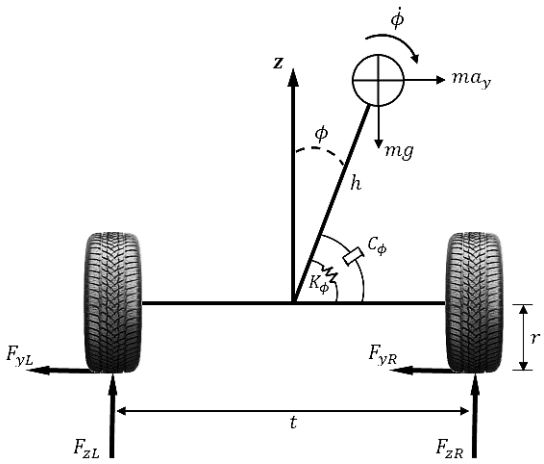

Figure 2: Behind view of the two-track model in vertical plane

Figure 3: Free body diagram of the wheel during braking

The governing equations associated with the angular and translational motions are as below [20]:

$$\ddot{\phi} = \frac{F_{yT}h\cos\phi + mgh\sin\phi - C_\phi\dot{\phi} - K_\phi\phi + \dot{\psi}^2(I_{yy}-I_{zz})\sin\phi\cos\phi}{I_{xx}} \quad (1)$$

$$\ddot{\psi} = \frac{M_T - F_{xT}h\sin\phi - 2(I_{yy}-I_{zz})\sin\phi\cos\phi\dot{\phi}\dot{\psi}}{I_{yy}\sin^2\phi + I_{zz}\cos^2\phi} \quad (2)$$

[DOI: 10.22068/ase.2020.544]

$$\dot{u} = \frac{F_{xT}}{m} + v\dot{\psi} - hsin\phi\left(\frac{M_T - F_{xT}h\,sin\phi - 2(I_{yy}-I_{zz})sin\phi cos\phi\dot{\phi}\dot{\psi}}{I_{yy}sin^2\phi + I_{zz}cos^2\phi}\right) \quad (3)$$

$$\dot{v} = \frac{F_{yT}}{m} - u\dot{\psi} - hsin\phi cos\phi\dot{\psi}^2 + \frac{h}{I_{xx}}(F_{yT}h\,cos\phi + mgh\,sin\phi - C_\phi\phi - K_\phi\dot{\phi} + \dot{\psi}^2(I_{yy} - I_{zz})sin\phi\,cos\phi) \quad (4)$$

Where h, m and I_{ii} outline the distance from the roll center to the C.G., the vehicle mass and the moment inertia about the ith axis, correspondingly.

It should be noted that the reference [20] used the linear forms of the equations. However, in this paper, we study the nonlinear form the equations. Also, the equations governing the motions of the wheel can be written as [22]:

$$rF_x^{fl} - T_b^{fl} = I_w\dot{\omega}^{fl} \quad (5)$$

$$rF_x^{fr} - T_b^{fr} = I_w\dot{\omega}^{fr} \quad (6)$$

$$rF_x^{rl} - T_b^{rl} = I_w\dot{\omega}^{rl} \quad (7)$$

$$rF_x^{rr} - T_b^{rr} = I_w\dot{\omega}^{rr} \quad (8)$$

where ω is the angular velocity of the wheel, I_w is the total moment of inertia of the wheel, $T_b[T_b^{fl}\ T_b^{fr}\ T_b^{rl}\ T_b^{rr}]$ is the braking torque, r is the wheel radius and $F_x$is the longitudinal tire force. Hereinafter, the superscripts and the subscripts *fl*, *fr*, *rl* and *rr* illustrate the front left, front right, rear left and rear right, respectively.

2.1. Nonlinear tire Modeling

In the present study, the nonlinear combined slip tire model so-called *Pacejka Magic Formula* [23 and 24] has been used for simulating the behavior of tire. The longitudinal force F_x is generated due to the longitudinal slip, λ, while, the lateral force F_y is produced because of the lateral slip, α. The general form of the *Magic Formula* is as follows [23 and 24]**:**

$$y = D\,sin[C\,\arctan\{B\,z - E(arctanBz)\}] \quad (9)$$

where z is the input variable for the longitudinal or the lateral slip, y stands for the output variable of F_x, F_y or probably M_z. Also, *B*, *E*, *C* are the stiffness, curvature, shape factors, respectively and D denotes the maximum value. According to the vehicle dynamics as shown in Figure 4, the normal forces of each of the wheels can be obtained as follows

$$F_{z_{fl}} = \frac{F_{zF}}{2} + \Delta F_{zF} \quad (10)$$

$$F_{z_{fr}} = \frac{F_{zF}}{2} - \Delta F_{zF} \quad (11)$$

$$F_{z_{rl}} = \frac{F_{zR}}{2} + \Delta F_{zR} \quad (12)$$

$$F_{z_{rr}} = \frac{F_{zR}}{2} - \Delta F_{zR} \quad (13)$$

The two components of the normal load, i.e. static and dynamic loads which are initiated by the distribution of the vehicle mass and load transfer during braking, respectively, can be obtained according to equations (14) and (15):

$$F_{zF} = \frac{mglr}{lf+lr} - \frac{mH}{lf+lr}\ddot{x} = \frac{mglr - mH\dot{u}}{lf+lr} \quad (14)$$

$$F_{zR} = \frac{mglf}{lf+lr} + \frac{mH}{lf+lr}\ddot{x} = \frac{mglf + mH\dot{u}}{lf+lr} \quad (15)$$

in which F_{zF}, F_{zR}, m, H, lf, lr and $\ddot{x}(\dot{u})$ denote the front axle normal load, rear axle normal load, vehicle mass, height of the center of gravity, distance from the front wheels to the center of gravity, distance from the rear wheels to the center of gravity and the longitudinal acceleration, respectively. Considering roll effects, dynamic components can be modified as follows:

$$\Delta F_{zF} = \frac{m\ddot{y}Hlr}{t(lf+lr)} - \frac{K_{\phi_f}\phi + C_{\phi_f}\dot{\phi}}{t} \quad (16)$$

$$\Delta F_{zR} = \frac{m\ddot{y}Hlf}{t(lf+lr)} - \frac{K_{\phi_r}\phi + C_{\phi_r}\dot{\phi}}{t}\ ,$$

$$(K_{\phi_f}{=}K_{\phi_r} = \frac{K_\phi}{2},\ C_{\phi_f}{=}C_{\phi_r} = \frac{C_\phi}{2}) \quad (17)$$

where ΔF_{zF}, ΔF_{zR}, t and $\ddot{y}(\dot{v})$ are the difference between the normal load of right and left sides related to the front axle, the difference between the normal load of right and left sides related to rear axle, the track width and lateral acceleration, correspondingly.

[DOI: 10.22068/ase.2020.544]

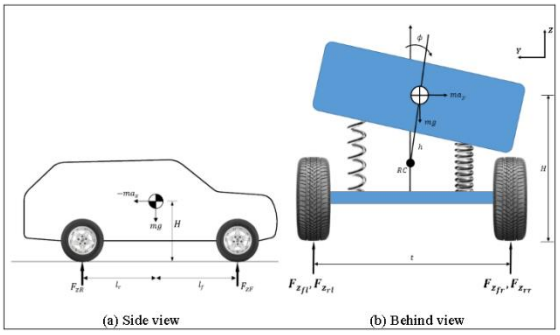

Figure 4: Obtained resultant normal loads corresponding to each tire: (a) Side view of a schematic of the vehicle; (b) Behind view of force analysis of a simple vehicle in cornering (1-DOF roll model)

By considering Figure 5, the total forces and moments which have been previously used in equations (1) to (4), can be obtained by [20 and 23]:

$$F_{xT} = F_x^{rl} + F_x^{rr} + \left(F_x^{fl} + F_x^{fr}\right)cos\delta - (F_y^{fl} + F_y^{fr})sin\delta \quad (18)$$

$$F_{yT} = F_y^{rl} + F_y^{rr} + \left(F_y^{fl} + F_y^{fr}\right)cos\delta - (F_x^{fl} + F_x^{fr})sin\delta \quad (19)$$

$$M_T = \left(F_y^{fl} + F_y^{fr}\right)lfcos\delta - \left(F_y^{rl} + F_y^{rr}\right)lr + \left(F_x^{fl} + F_x^{fr}\right)lfsin\delta + (F_x^{rr} + F_x^{fr}cos\delta + F_y^{fl}sin\delta - F_x^{rl} - F_x^{fl}cos\delta - F_y^{fr}sin\delta)t/2 \quad (20)$$

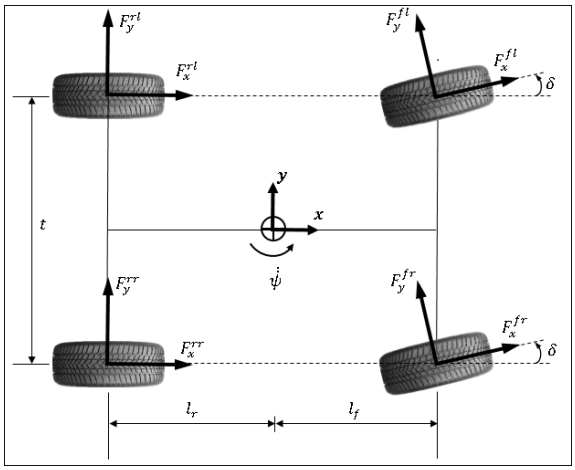

Figure 5: Planar model, displaying the longitudinal and lateral forces of tires

In order to present a more precise investigation, block diagram representation of the nonlinear eight-DOF dynamic model including a tire modeling and a chassis modeling, is revealed in Figure 6 in which the actuator inputs are the four torque braking, as well as the steering angle. The outputs of the system are the vehicle states.

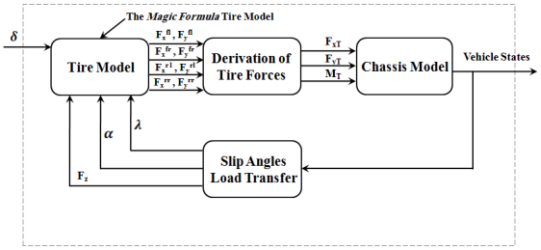

Figure 6: The block diagram of our developed nonlinear eight-DOF dynamic model including a tire modeling and a chassis modeling

3. Control System

3.1. SMC-based stabilizing controller

This subsection presents a nonlinear control system on the basis of SMC to prevent the vehicle rollover. Since the governing dynamic equations of the vehicle are nonlinear, it is appropriate to deploy a nonlinear control design methodology. The SMC is a powerful theory that lends itself for designing robust controllers [25 and 26]. The ability of this method is that a robust controller designed in confronting uncertainties and disturbances with determined bounds. The purpose of control system includes two parts. Firstly, vehicle rollover should be avoided by minimum braking torque. Secondly, the roll angle must be stabilized. We adopt the MUGA method [27 and 28] to optimally tune the parameter of the sliding controller, in spite of the conflict in goals. In the next subsection, this matter is elaborated in detail and the conflicting objective functions are introduced.

Using equations (1) to (8), the state-space representation of the nonlinear dynamic system can be expressed as:

$$\dot{x} = f(x) + bu \quad (21)$$

Where :

[DOI: 10.22068/ase.2020.544]

$x = [x_1\ x_2\ x_3\ x_4\ x_5\ x_6\ x_7\ x_8\ x_9\ x_{10}]^T \in \Re^{10}$ is the vehicle states vector. States x_1, x_2, x_3, x_4, x_5, x_6, x_7, x_8, x_9 and x_{10} are expressed as roll angle(ϕ), roll rate($\dot{\phi}$), yaw angle(ψ), yaw rate($\dot{\psi}$), longitudinal velocity(u), lateral velocity(v), angular velocity of the fl wheel(ω^{fl}), angular velocity of the fr wheel(ω^{fr}), angular velocity of the rl wheel(ω^{rl}) and angular velocity of the rr wheel(ω^{rr}), respectively. u defines the vector of system control inputs. b denotes matrices with suitable dimension. The state-space representation equations related to equations (1) to (8) are as follows:

$$\dot{x}_1 = x_2 \tag{22}$$

$$\dot{x}_2 = \frac{F_{yT}h\,cosx_1 + mgh\,sinx_1 - C_\phi x_1 - K_\phi x_2 + {x_4}^2(I_{yy}-I_{zz})sinx_1\,cosx_1}{I_{xx}} \tag{23}$$

$$\dot{x}_3 = x_4 \tag{24}$$

$$\dot{x}_4 = \frac{M_T - F_{xT}h\,sinx_1 - 2(I_{yy}-I_{zz})sinx_1 cosx_1 x_2 x_4}{I_{yy}sin^2x_1 + I_{zz}cos^2x_1} \tag{25}$$

$$\dot{x}_5 = \frac{F_{xT}}{m} + x_6 x_4 - hsinx_1\left(\frac{M_T - F_{xT}h\,sinx_1 - 2(I_{yy}-I_{zz})sinx_1 cosx_1 x_2 x_4}{I_{yy}sin^2x_1 + I_{zz}cos^2x_1}\right) \tag{26}$$

$$\dot{x}_6 = \frac{F_{yT}}{m} - x_5 x_4 - hsinx_1 cosx_1 {x_4}^2 + \frac{h}{I_{xx}}(F_{yT}h\,cosx_1 + mgh\,sinx_1 - C_\phi x_1 - K_\phi x_2 + {x_4}^2(I_{yy}-I_{zz})sinx_1\,cosx_1) \tag{27}$$

$$\dot{x}_7 = \frac{rF_x^{fl} - T_b^{fl}}{I_w} \tag{28}$$

$$\dot{x}_8 = \frac{rF_x^{fr} - T_b^{fr}}{I_w} \tag{29}$$

$$\dot{x}_9 = \frac{rF_x^{rl} - T_b^{rl}}{I_w} \tag{30}$$

$$\dot{x}_{10} = \frac{rF_x^{rr} - T_b^{rr}}{I_w} \tag{31}$$

Based upon the SMC technique, the switching surface S is defined as follows:

$$S = \tilde{x} + k\int \tilde{x} \tag{32}$$

where $k = diag([k_1\ k_2\ k_3\ k_4\ k_5\ k_6\ k_7]) \in \Re^{7\times7}$ is SMC gain. The error between the actual value and the desired value reads as:

$$\tilde{x} = x_c - x_c^d \tag{33}$$

in which $x_c = [x_1\ x_2\ x_4\ x_7\ x_8\ x_9\ x_{10}]^T \in \Re^7$ is the control states vector. Also, $x_c^d \in \Re^7$ is the desired states vector. A control law could be obtained so that $\dot{S} = 0$. Differentiating equation (32) with respect to time gives the derivative form:

$$\dot{S} = \dot{\tilde{x}} + k\tilde{x} \tag{34}$$

Substituting $\dot{\tilde{x}} = f(\tilde{x}) + bu$ into equation (34), according to equation (21), we arrive at:

$$\dot{S} = f(\tilde{x}) + bu + k\tilde{x} = 0 \tag{35}$$

Hence, the control law is achieved as:

$$u_{eq} = -b^{-1}k\tilde{x} - b^{-1}f(\tilde{x}) \tag{36}$$

Based on the process illustrated by equations (21) to (36), the equivalent braking torques of the four wheels are estimated. Figure 7 represents the block diagram of the control system considered in this work.

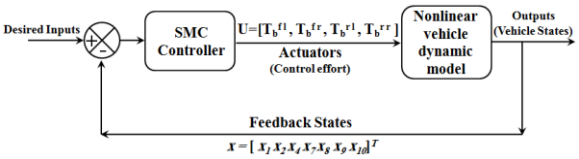

Figure 7: Configuration of the proposed optimized sliding mode control system

3.2. Multi-objective parameter tuning

The heuristic sliding mode controller gains are required to be chosen properly for rollover prevention of a full vehicle dynamic model with an eight-DOF as presented in the "System modeling" section. As an application of our previously developed MUGA algorithm, represented in Figure 8, we adopt it to optimally tune the parameter of the sliding mode controller, in spite of the conflict in objectives. More detailed description of MUGA can be found in [27 and 28]. Therefore, the MUGA is utilized to find the gains of SMC with respect to the two conflicting objective functions, namely, absolute area under the curve of roll angle over time and area under the curve of total braking torque over time. Two conflicting objective functions are formulated as follows:

[DOI: 10.22068/ase.2020.544]

$$f_1 = \int |\varphi(t)| dt \quad (37)$$

$$f_2 = \sum_{i=1}^{4} u_i \quad (38)$$

where $u_1 = \int T_b^{fl}\, dt\, .u_2 = \int T_b^{fr}\, dt.u_3 = \int T_b^{rl}\, dt$ and $u_4 = \int T_b^{rr}\, dt$.

Evidently, it can be noted that these objective functions have to be minimized, simultaneously. The vector $[k_1, k_2, k_3, k_4, k_5, k_6, k_7]$ is the vector of selective gains of SMC (design variables). This demonstrates that by choosing different amounts for the selective gains, which is changeable in each one of two mentioned objective functions. in this study, we are interested in choosing values for selective gains to minimize these objective functions. It is clear that this is an optimization problem with two objective functions and seven decision variables. The input variables are set to be in the range $k_i \in [0,1000](i = 1-7)$.

4. Simulation results and discussion

The aim of the simulation scenarios presented here is the application of the MUGA-based SMC described in the "Control system" section to avoid the rollover of our developed vehicle dynamic model. Table 1 represents list of the numerical values of the relevant parameters of the SUV model used in the simulation.

Table 1: The values of fixed parameters of the SUV model [14]

Fixed parameter	Value
M	1146.6 kg
I_{xx}	442 kg m^2
I_{yy}	1302 kg m^2
I_{zz}	1302 kg m^2
l_f	0.88 m
l_r	1.32 m
H	0.51m
C_ϕ	1000 N.m.s/rad
K_ϕ	60000 N.m/rad
r	0.39 m
T	1.76 m

The initial vehicle speed is considered to be 80 km/h (equivalently 22.22 m/s) and the steering wheel input is shown in Figure 8 [29]. The peak angle of this maneuver is assumed to be 221 deg. This maneuver as an untripped rollover maneuver, tries to maximize the vehicle roll angle under the dynamic motion condition (see [2] for more details regarding the Fishhook maneuver). The consideration of this maneuver for the steering input, simulates very hard and critical condition which rarely happens in the real. Therefore, the results achieved can be practical in the real state where the intensity of maneuvers is lower than this.

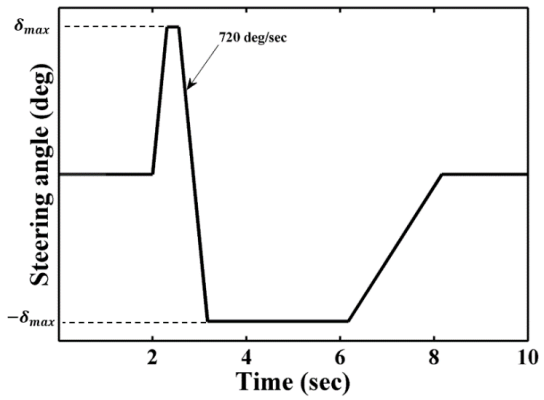

Figure 8: Fishhook steering input

Optimum Pareto design of SMC is now deployed via the MUGA process. In case of optimum design of sliding mode controller from the multi-criteria viewpoint, the specifications required to perform the utilized optimization algorithm in this work are given in Table 2.

Table 2: Required parameters to perform the MUGA process

Parameter	Value
Population	80
Crossover	0.95
Mutation	0.1
Generation	240

With the implementation of the genetic algorithm program, 71 non-dominate optimal design points which are called Pareto points are extracted from the distribution of two objective functions, which are demonstrated in the Figure 9. As shown in the Figure 9, the points No.1, No.3 and No.2 are the important points of the Pareto front.

[DOI: 10.22068/ase.2020.544]

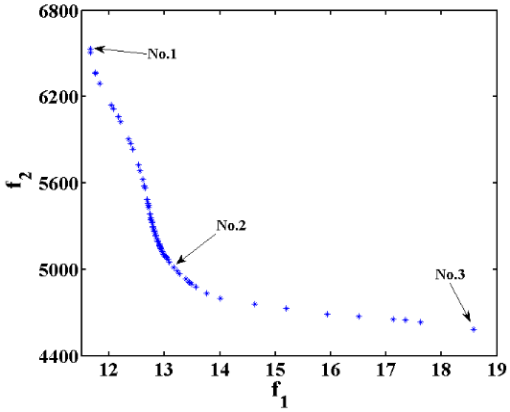

Figure 9: Pareto front of the optimum controller design

However, all the points obtained in the Figure 9 are optimal, and each of them can be selected as a best from a designer's point of view. But point No.2 could be a better one to design from the point of view in both objective functions and is selected as a design compromise point. In such a way, by moving from No.1 to No.2, without a significant increase in the objective function of the car roll angle, a significant reduction, about 78%, is seen in the objective function of control effort. Without applying the multi-objective optimization such an optimal design point cannot be achievable. Since all the points obtained in the Pareto front which are shown in Figure 9 are optimal, for each of them the car does not overturn. So by moving on the Pareto curve, the simulation results of points No.1, No.3 and No.2 are compared, respectively. Design variables and objective functions are presented in Table 3.

Table 3: The objective functions and the values of control parameters at the optimum points No.1, No.3, and No.2

Optimum design point	**No.1**	**No.2**	**No.3**
f_1	11.66	13.16	18.58
f_2	6533	5013	4582
Design variable k_1	248.46	252.35	243.20
Design variable k_2	145.72	144.19	143.54
Design variable k_3	105.34	102.83	101.21
Design variable k_4	354.60	352.21	351.86
Design variable k_5	323.17	305.46	310.52
Design variable k_6	349.91	184.71	179.01
Design variable k_7	260.47	219.38	215.23

Figures 10 to 15 show the time responses of the point No.2 with and without the controller. The obtained results illustrate that the rollover happens right after attainment of the peak value of the second steering step, while the controller is deactivated. In Figure 10, the sever instability of the roll dynamics can be observed clearly in the uncontrolled mode.

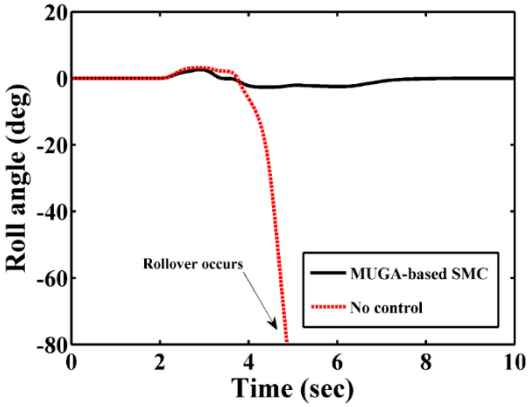

Figure 10: Time responses of roll angle

Moreover, the rapid growth of both the roll angle and the roll rates, as illustrated by Figures 10 and 11, reveal that they are the most important parameters in controller design. Further to this, the activating controller indicates that the roll angle is limited to about 5 degrees in the worst motion condition while it reaches to 80 degrees in the case of deactivated control. In addition, the roll angle becomes zero at the end of maneuver.

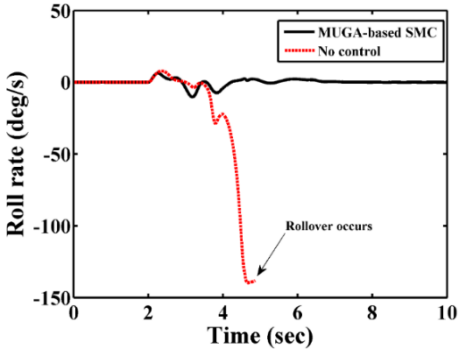

[DOI: 10.22068/ase.2020.544]

Figure 11: Time responses of roll rate

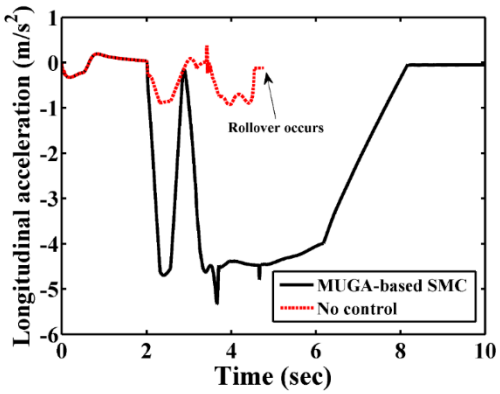

Figure 12: Time responses of longitudinal acceleration

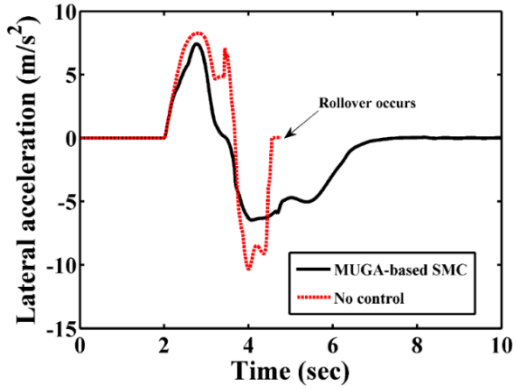

Figure 13: Time responses of lateral acceleration

As there is no speed control to maintain a constant speed, it can be observed that velocity reduces to 15 km/h at the end of the Fishhook maneuver, as depicted in Figure 14.

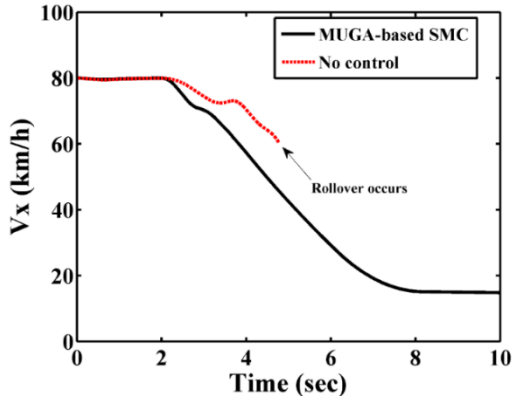

Figure 14: Time responses of longitudinal velocity

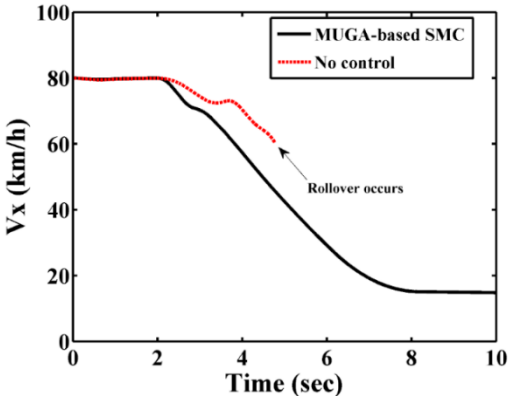

Figure 15: Time responses of lateral velocity

In order to avoid rollover, the differential braking strategy for applied torque distribution on the left or side wheels is considered to be as: if the sign of steering wheel input is positive, only the distributed torques on the right wheels are utilized, otherwise, the distributed torques on the left wheels are used [14]. The torque fades away as the steering reaches to zero [14]. Figure 16 depicts the controller inputs of the trade-off design point No.2. This figure shows that smooth brake torques for all wheels are obtained by proposed strategy.

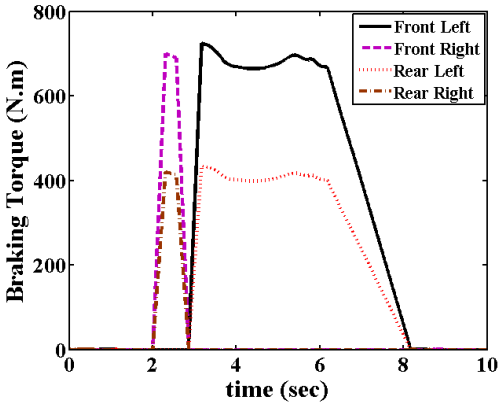

Figure 16: Braking torque of the trade-off optimum design point No.2

According to Figures 10 and 13, the roll angle and the lateral acceleration are decreased. This matter is due to the optimum braking torque input of the optimum designed controller, as depicted

[DOI: 10.22068/ase.2020.544]

in Figure 16. It is found that the highest value of the obtained braking torque is lower than that reported by [14 and 22]. The vehicle trajectory corresponding to the point No.2 in the inertial xy plane is depicted in Figure 17.

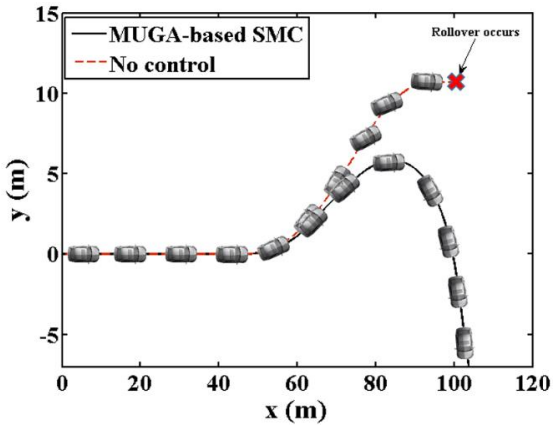

Figure 17: Trajectories of vehicle undergoing the Fishhook steering input

It is clear that the vehicle lies on the desired trajectory associated with the fishhook steering wheel input when the controller is active.

Table 4 provides a comparison between the present simulation results and those presented in [14 and 17]. It is very evident from this table that the highest roll angle and lateral acceleration reduce around approximately 7٪ and 6٪ during the first steering action and also about 30٪ and 25 ٪during the second steering action in comparison with [14], respectively. Also, it can be seen from this table that the maximum value of roll angle and lateral acceleration obtained in this paper improve about 21٪ and 19٪ during the first steering action and also about 26٪ and 31٪ during the second steering action than those in [17].

Table 4: Comparison of the peak values of the roll angle lateral acceleration with the available results in the literature

	Peak roll angle (first steering)	**Peak lateral acceleration (first steering)**	**Peak roll angle (second steering)**	**Peak lateral acceleration (second steering)**
Present study	2.6 deg	7.42 m/s^2 (equivalently 0.76 g)	2.7 -deg	**-6.43 m/s^2 (equivalently 0.66 g)**
Ref. [14]	2.8 deg	7.9 m/s^2	-3.9 deg	**-8.5 m/s^2**
Ref. [17]	3.3 deg	0.94 g	-3.6 deg	**-0.96 g**

5. Conclusion

The current research focuses on an eight-DOF two-track dynamic system and designs an active safety controller to reduce the occurrence of lateral dynamic instability of vehicle-type rollover on the basis of differential braking with optimized distribution of braking torques. The artificial intelligence-based MUGA is implemented and the sliding mode controller is optimally tuned to achieve the desired trade-off in lateral stabilization of the sport utility vehicle. In particular, seven gains of related control law were optimized considering two simultaneous conflicting objective functions. The multi-criteria optimization of SMC led to the discovering important trade-offs among those objective functions which would not have been found otherwise. The simulation results verify that by applying multi-criteria optimum sliding controller, the roll stability of vehicle can be considerably improved in spite of increasing lateral acceleration. Since the consideration of Fishhook maneuver for the steering input, simulates very hard and critical condition which rarely happens in real, therefore, the results achieved can be practical in the real state where the intensity of maneuvers is lower than this. This testifies to the practicality of the designed optimal controller.

Acknowledgments

The authors acknowledge the financial support from the Lahijan branch, Islamic Azad University.

References

[1] National Highway Traffic Safety Administration. Rollover characteristic, http://www.safercar.gov/Rollover (2008).

[2] G. J. Frokenbrock, W.R. Garrott, B. C. Hara, A comprehensive experimental examination of test maneuvers that may induce on-road, untripped, light vehicle rollover - phase IV of NHTSA's light vehicle rollover research

[DOI: 10.22068/ase.2020.544]

program. Report for the US Department of Transportation, Report no. DOT HS 809 513, (2002).

[3] National Center for Statistics & Analysis. Motor vehicle traffic crash fatality counts and estimates of people injured for 2007. Report no. DOT HS 811 034, (2009).

[4] Fatality Analysis Reporting System (FARS), http://www-fars.nhtsa.gov, (2009).

[5] B. Frechede, A. S. Mclntosh, R. Grzebieta, M. R. Bambach, Characteristics of single vehicle rollover fatalities in three Australian states (2000-2007), Accident Analysis and Prevention, Vol.43, No.3, (2011), pp.804-812.

[6] S. Anwar, Generalized predictive control of yaw dynamics of a hybrid brake-by-wire equipped vehicle, Mechatronics, Vol.15, No.9, (2005), pp. 1089−1108.

[7] S. Anwar, Anti-lock braking control of a hybrid brake-by-wire system. Proceedings of the Institution of Mechanical Engineers, Part D: Journal of Automobile Engineering, Vol.220, No.8, (2006), pp.1101−1117.

[8] L. Wang, N. Zhang, H. Du, Design and experimental investigation of demand dependent active suspension for vehicle rollover control, Proceedings of IEEE Conference on Decision and Control, (2009), pp.5158-5163.

[9] M. Moavenian, S. Sadeghi namaghi, An adaptive modified fuzzy-sliding mode longitudinal control design and simulation for vehicles equipped with ABS system, International Journal of Automotive Engineering, Vol.9, No.1, (2019), pp. 2895-2907.

[10] A. Harifi, F. Rashidi, F. Vakilpoor Takaloo, Design of an Adaptive Fuzzy Controller for Antilock Brake Systems, International Journal of Automotive Engineering, Vol.10, No.1, (2020), pp. 3158-3166.

[11] S. Di Cairano, H. E. Tseng, D. Bernardini, A. Bemporad, Vehicle yaw stability control by coordinated active front steering and differential braking in the tire sideslip angles domain, IEEE Transactions on Control Systems Technology, Vol.21, No.4, (2013), pp. 1236−1248.

[12] M. Doumiati, O. Sename, L. Dugard, J. Martinez, P. Gaspar, Z. Szabo, Integrated vehicle dynamics control via coordination of active front steering and rear braking, European Journal of Control, Vol.19, No.2, (2013), pp. 121-143.

[13] J. Rezapour, B. Bahrami Joo, A. Jamali, N. Nariman-zadeh, Multi-objective Optimization of Nonlinear Controller for Untripped Rollover Prevention of an 8-dof Vehicle Dynamic Model, Applied Mechanics and Materials, Vol.775, (2015), pp. 347-351.

[14] S. Yim, Design of a robust controller for rollover prevention with active suspension and differential braking, Journal of Mechanical Science and Technology, Vol.26, No.1, (2012), pp.213-222.

[15] R. Tchamna, I. Youn, Yaw rate and side-slip control considering vehicle longitudinal dynamics, International Journal of Automotive Technology, Vol.14, No.1, (2013), pp. 53-60.

[16] H. Imine, T. Madani, Sliding-mode control for automated lane guidance of heavy vehicle, International Journal of Robust and Nonlinear Control, Vol.23, No.1, (2013), pp. 67-76.

[17] S. Yim, Y. Park, Design of rollover prevention Controller with linear matrix inequality based trajectory sensitivity minimization, Vehicle System Dynamics, Vol.49, No.8, (2011), pp.1225-1244.

[18] J. Kang, J. Yoo and K. Yi, Driving control algorithm for maneuverability, lateral stability, and rollover prevention of 4WD electric vehicles with independently driven front and rear wheels, IEEE Transactions on Vehicular Technology, Vol.60, No.7, (2011), pp.2987-3001.

[19] C. Zong, T. Zhu, C. Wang, H. Liu, Multi-objective stability control algorithm of heavy tractor semi-trailer based on differential braking,

[DOI: 10.22068/ase.2020.544]

Chinese Journal of Mechanical Engineering, Vol.25, No.1, (2012), pp. 88-97.

[20] B. Schofield, Vehicle dynamics control for rollover prevention, PhD dissertation, Department of Automatic Control, Lund University, (2006).

[21] S. Westhuizeh, P. Els P, Slow active suspension control for rollover prevention, Journal of Terramechanics, Vol.50, No.1, (2013), pp.29-36.

[22] M. Mirzaei, H. Mirzaeinejad, Optimal design of a non-linear controller for anti-lock braking system, Transportation Research Part C, Vol. 24, (2012), pp.19-35.

[23] H. B. Pacejka, Tyre and vehicle dynamics. 3th ed. Elsevier, (2012).

[24] H. B. Pacejka, I. J. M. Besselink, Magic Formula Tyre Model with Transient Properties. Vehicle System Dynamics: International Journal of Vehicle Mechanics and Mobility, Vol.27, (1997), pp.234-249.

[25] J. Rezapour, M. Sharifi, N. Nariman-Zadeh, Application of fuzzy sliding mode control to robotic manipulator using multi-objective genetic algorithm. In: IEEE international symposium on innovations in Intelligent Systems and Applications (INISTA 2011), (2011), pp. 455-459.

[26] A. Pezhman, J. Rezapour, M. J. Mahmoodabadi, An optimal hybrid adaptive controller based on the multi-objective evolutionary algorithm for an under-actuated nonlinear ball and wheel system, Journal of Mechanical Science and Technology, Vol.34, No.4, (2020), pp.1723-1734.

[27] J. Rezapour, B. Bahramijoo, A. Jamali, N. Nariman-zadeh, Robust multi-objective controller design for vehicle rollover prevention, International Journal of Automotive Engineering, Vol.4, No.4, (2014), pp. 846-856.

[28] N. Nariman-Zadeh, M. Salehpour, A. Jamali, E. Haghgoo, Pareto optimization of a five-degree of freedom vehicle vibration model using a multi-objective uniform-diversity genetic algorithm (MUGA), Engineering Applications of Artificial Intelligence, Vol.23, No.4, (2010) pp. 543-551.

[29] G. J. Frokenbrock, W. R. Garrott, Testing the dynamic rollover resistance of two 15-passenger vans with multiple load configurations. Report for the US Department of Transportation, Report no.DOT HS 809 704, (2004).

[DOI: 10.22068/ase.2020.544]